Publication IV

Ouni T., Honkela M., Kolah A. and Aittamaa J., Isobutene dimerisation in a miniplant-scale reactor. Accepted for publication in *Chem. Eng. Process* in *October 2005.*

Available online at www.sciencedirect.com
SCIENCE DIRECT®
Chemical Engineering and Processing xxx (2005) xxx–xxx
Chemical Engineering and Processing
www.elsevier.com/locate/cep

Isobutene dimerisation in a miniplant-scale reactor

Tuomas Ouni*, Maija Honkela, Aspi Kolah, Juhani Aittamaa

Helsinki University of Technology, Department of Chemical Technology, P.O. Box 6100, 02015 HUT, Espoo, Finland

Received 31 January 2005; received in revised form 13 June 2005; accepted 30 September 2005

Abstract

A miniplant-scale tubular reactor with an inside diameter of 0.016 m and length of 1.3 m was used to produce 2,4,4-trimethylpentene (isooctene) by dimerizing 2-methylpropene (isobutene). The reaction took place in liquid phase in presence of a solid macroporous ion exchange resin catalyst. The reactor system included an external heating coil with temperature-controlled heat transfer fluid and an axial internal thermowell for temperature probes.

The reaction was studied with two reactors in series, varying the feed compositions and temperature set points of the reactors. In addition to the feed and product compositions, the temperature profiles of the reactor were measured.

A two-dimensional pseudohomogeneous model for the catalyst bed and separate models for the reaction kinetics and liquid phase activity coefficients were combined with a hardware-specific model, which took both the heating coil and the thermo well into account. Kinetic models for the reactions involved were liquid-phase activity-based, Langmuir–Hinselwood-type models.

The simulation model predicted well the measured axial temperature and concentration gradients in the reactor. Calculations revealed significant radial temperature variations inside the catalyst bed, necessitating the use of a two-dimensional model in reactor simulations.

Conversions and selectivities of diisobutene given by the model matched well with those obtained from the experiments. Once-through yields up to 65% were measured for diisobutene.

Keywords: Catalytic; Reactor; Modelling; Isobutene; Dimerisation

1. Introduction

Methyl *tert*-butyl ether (MTBE, 2-methoxy-2-methylpropane), once the blue eye chemical of the chemical industry and in the last decade having been labelled as the fastest growing chemical in the world, is currently under tremendous scrutiny and pressure in the United States from environmental regulation agencies and public to decrease or totally eliminate its use from the gasoline pool. Since the last 20 years, MTBE has been blended into gasoline and it is an efficient way for refineries to meet the regulations for oxygenated and reformulated gasoline.

Ground water and surface water contamination associated with MTBE from leaking underground tanks is the cause of the current controversy as between 5 and 10% of ground water in areas using MTBE blended gasoline have detectable levels of MTBE. As a consequence, a ban on MTBE took effect from January 2004 in California after granting a 1-year waiver [1,2], and several other states in USA are predicted to follow California's action.

Of the various potential substitutes to MTBE, isooctane is one of the leading contenders. Isooctane is synthesised from isobutylene by selective dimerisation to form isooctene, followed by hydrogenation. In locations where the olefin content of gasoline is not limited, isooctene can be directly blended into the gasoline pool. Isooctane has numerous advantages, its properties being high octane number and zero content of aromatics, sulphur and low vapour pressure and for the MTBE producing refineries it has the decisive advantage of necessitating a moderate revamp of the already existing refinery facilities. Moreover, MTBE has

Abbreviations: CSTR, continuously stirred tank reactor; DIB, diisobutene; DIPPR, the design institute for physical properties; FCC, fluid catalytic cracking; GC, gas chromatograph; LLE, liquid–liquid equilibrium; MTBE, methyl-*tert*-butyl ether, 2-methoxy-2-methylpropane; ODE, ordinary differential equation; PDE, partial differential equation; TBA, *tert*-butyl alcohol, 2-methyl-2-propanol; TMP-1, 2,4,4-trimethyl-1-pentene; UNIFAC, universal quasi-chemical functional group activity coefficient; VLE, vapour–liquid equilibrium

* Corresponding author. Tel.: +358 9 451 2636; fax: +358 9 451 2694.
E-mail address: tuomas.ouni@hut.fi (T. Ouni).

0255-2701/$ – see front matter © 2005 Published by Elsevier B.V.
doi:10.1016/j.cep.2005.09.005

been a major consumer of isobutylene from C4 hydrocarbon stock and its phase out will cause a major decline in the downstream consumption of isobutylene from fluid catalytic cracking and steam cracking product streams.

2-Methylpropene (isobutene) is dimerised into 2,4,4-trimethylpentene (isooctene) in presence of a solid ion exchange resin catalyst. Tri- and tetraisobutenes are formed as side products [3]. Industrially, the feed to the reactors can be a isobutene containing C4-stream from different sources, e.g. the similar feed as in MTBE units can be used. Here, a mixture of isobutene and inert components, mainly isobutane, is used. *tert*-Butyl alcohol (2-methyl-2-propanol, TBA) is used in the feed as a selectivity-controlling agent [4]. Without TBA, the reaction kinetics favour the forming of larger, C12 and C16 oligomers of isobutene [5].

The dimerisation reaction is highly exothermic and heat must be removed to avoid temperature rise leading to the formation of higher oligomers [3,6]. These oligomers have relatively high molecular weight and boiling point and are not suitable for blending into the gasoline pool. Moreover, the catalyst deactivation increases at temperatures above 393 K, when the sulphonic groups of the resin start to disengage and the catalyst loses its surface activity. Dimerisation is here studied in a miniplant-scale tubular reactor.

The concept of miniplant is placed between laboratory scale and bench scale equipment. Miniplant-scale equipment is used to test thermodynamical phenomena and individual hardware components, and the knowledge obtained is further transferred into industrial scale. The objective of miniplant testing is to speed up process development by reducing the intermediate testing stages between laboratory scale and industrial scale. Miniplant hardware costs as well as utility and chemical costs are usually relatively moderate which makes the technology available for, e.g. universities and small research institutes. Also safety issues are more easily dealt with when small-scale equipment is used.

A miniplant was build at the Helsinki University of Technology (HUT) for process design purposes. The main units of the miniplant are distillation columns and tubular reactors, supplemented with necessary accessories such as pipelines, vessels, pumps and automation. The feed rate can be varied between 0.15 and 0.5 kg/h. The HUT hardware details are further discussed by Lievo et al. [7].

The reactors of the HUT miniplant are single-tube, externally cooled reactors with an axial thermowell. With external cooling the operation window of the reactors can be expanded, and the reaction can be studied at various conditions. However, low tube-to-particle diameter ratio, external cooling and thermowell must be rigorously modelled to find the physicochemical phenomena behind the hardware specific phenomena. This is the ideology behind miniplant: modelling the small-scale equipment as accurately as possible and finding models for various hardware-independent phenomena to be applied in larger scale. In terms of scale-up, this allows one or two steps to be left out in the design procedure thus speeding up the process development significantly in order to meet challenges and demands of the industry.

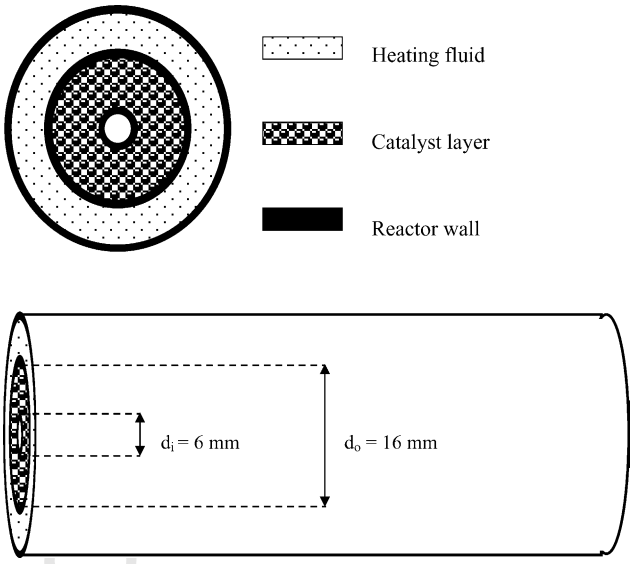

Fig. 1. A schematic representation of the tubular reactors used in the experiments.

The aim of the study is to combine thermodynamic and hardware-specific models concerning isobutene dimerisation in a catalytic tubular reactor. Dimerisation is studied under various reaction conditions, and individual model components are tailored to yield an accurate overall model, which can then be applied in optimising the operating conditions for isooctene production in a tubular catalytic reactor and the whole process.

2. Experimental

The experimental setup for the present study consisted of two fixed bed tubular reactors connected in series. The length of each tubular reactor is 1.3 m, constructed of SS-316L and designed for operating at pressures below 2.5 MPa and temperatures below 473 K. The internal diameter of the reactor is 16 mm having a concentric tube with a 6 mm outside diameter for placement of temperature measurement probes. Four temperature probes were placed in each reactor. During the experimental run the position of the temperature probes was changed in order to obtain the temperature profile over the whole catalyst bed. The estimated uncertainty for temperature measurements was ±0.1 K and for pressure measurements ±0.05 bar.

The heating of the reactor was controlled by an external annular heating jacket, connected to a heating/cooling bath. The flow direction of the heating fluid (technical white oil) was countercurrent to reactor fluid flow. A schematic representation of the reactor setup is presented in Fig. 1.

The flow direction in the reactors was downwards. The top portion of the reactor bed was packed with stainless steel springs to use it as heating section. The mass flow rates were measured by the use of weighing type balances on which the feed C4 gas bottles were placed. The estimated uncertainty for the balances was ±5 g. The liquefied C4-fraction was pumped by using of diaphragm type metering pumps obtained from Siemens. A syringe pump (Isco 260D) was used to add solvent, a mixture of TBA and 2,4,4-trimethylpentane (isooctane), to the reactor feed.

2.1. Materials

The feed was a technical mixture, which consisted of 39.68 wt% isobutene and inert hydrocarbons, mainly isobutane. Laboratory grade TBA of >99 wt% purity was obtained from MERCK-Schuhardt and isooctane of ≥99.5 wt% purity was obtained from Fluka Chemika AG. TBA and isooctane were used in a 50–50 wt% mixture as solvent for controlling the reaction rate and product selectivity. The catalyst was a commercial acidic ion-exchange resin consisting of a styrene–divinylbenzene-based support to which sulfonic acid groups had been added as active sites. It was obtained from Rohm and Haas and partially pre-dried before use. The average particle size $d_{P,ave}$ for the catalyst was 0.0008 m and it had a bulk density of 850 kg/m^3. The surface area of the dried catalyst was measured to be 37 m^2/g (measured by BET analysis) and the acid capacity 5.1 mmol/g (measured by titration) [8].

2.2. Analysis

Feed and product stream analysis was performed by using gas chromatograph (GC) techniques (HP 6850 Series) fitted with a flame ionisation detector. Temperature programming for the oven was used. Helium was used as the carrier gas at a flow rate of 20 ml/min. The GC results were corrected with a TBA response factor of 1.3.

2.3. Procedure

The set of experiments consisted of altogether 17 test runs, where two reactors were connected in series. The feed composition was monitored by measuring it with GC in 1 h intervals. The reactors were allowed to settle towards steady state for at least 4 h before the samples from the product stream were taken. During 1 day of test runs the conditions in the first reactor were held unchanged, and the set temperature was only changed in the second reactor. Two samples were taken from the product stream of both reactors for analysis.

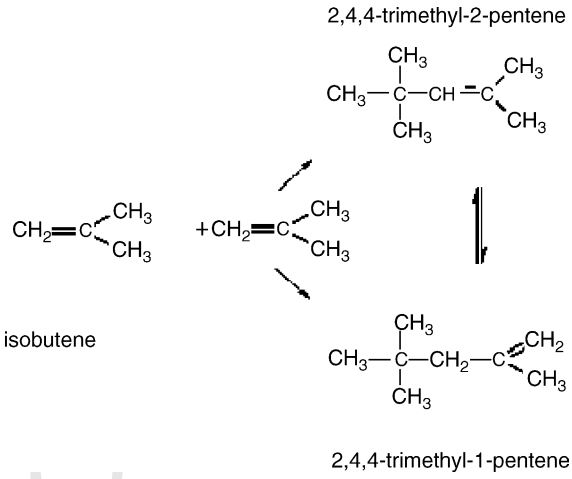

Scheme 1. Dimerisation reaction of isobutene.

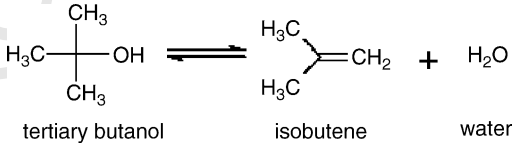

Scheme 3. TBA decomposition into water and isobutene.

3. Reactor model 1—equations for thermodynamic phenomena

3.1. Kinetic model

The three main reactions of concern in the dimerisation process are

- dimerisation of isobutene (Scheme 1);
- triisobutene formation from diisobutene and isobutene (Scheme 2, [9]) and;
- TBA decomposition into water and isobutene (Scheme 3).

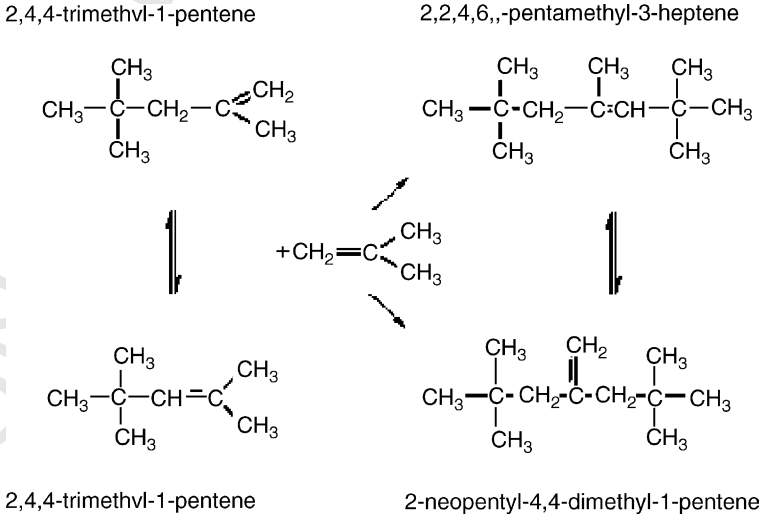

Scheme 2. Triisobutene formation reaction.

The kinetic model for isobutene dimerisation was developed by Honkela and Krause [10]. The model includes also the formation of triisobutene. The application range of the kinetic model is 333–393 K. Honkela and Krause tested mass transfer limitations both externally and internally. External mass transfer was studied by altering the mixer rotational speed in the CSTR used for the kinetic studies. Internal mass transfer for the catalyst was studied by performing kinetic tests with several catalyst particle sizes. According to Honkela and Krause, both internal and external mass transfer limitations in a CSTR were negligible.

Honkela and Krause studied also the formation of tetraisobutene in their article, but concluded that since the selectivity of tetraisobutene did not exceed 1.8% at any circumstances, inclusion of tetraisobutene production into the kinetic model is not necessary.

Both dimer and trimer formation rates have a strong dependence on the activity of TBA [3]. TBA has a reaction equilibrium with water and isobutene. Honkela et al. [8] studied the reaction at low (<18 wt%) TBA concentrations and in the absence of isobutene in the feed. The TBA concentrations of this study are well within this range. The temperature range of the study of Honkela et al. was from 333 to 363 K. Our conditions ranged from 323 to 361 K.

Summary of the kinetic equations along with their parameters is presented in Table 1.

Table 1
Kinetic equations for dimerisation and trimerisation of 2-methylpropene[a] and TBA decomposition[b] along with their parameter values

Reaction	
(1) Dimerisation of isobutylene	$r_{DIB} = \frac{k_{DIB} a_{IB}^2}{(a_{IB} + B_{TBA} a_{TBA})^2}$ $k_{DIB} = F_{ref,DIB}\, e^{-\frac{E_{DIB}}{R}\left(\frac{1}{T} - \frac{1}{T_{ref}}\right)}$, $T_{ref} = 373.15$ K
(2) Trimerisation of isobutylene	$r_{TRIB} = \frac{k_{TRIB} a_{IB} a_{TRIB}}{(a_{IB} + B_{TBA} a_{TBA})^3}$ $k_{TRIB} = F_{ref,TRIB}\, e^{-\frac{E_{TRIB}}{R}\left(\frac{1}{T} - \frac{1}{T_{ref}}\right)}$, $T_{ref} = 373.15$ K
(3) *tert*-Butyl alcohol decomposition	$r_{TBA} = \frac{k_{TBA}(a_{IB} a_{H_2O} - K_a a_{TBA})}{a_{TBA} + k_{H_2O} a_{H_2O}}$ $k_{TBA} = F_{ref,TBA}\, e^{-\frac{E_{TBA}}{R}\left(\frac{1}{T} - \frac{1}{T_{ref}}\right)}$, $T_{ref} = 343.15$ K $\ln K_a = -3111.9 \frac{1}{T/K} + 7.6391$

Reaction	Parameter	Value
(1)	$F_{ref,DIB}$	0.82
	E_{DIB}	30
(2)	$F_{ref,TRIB}$	0.065
	E_{TRIB}	1.8
(1) + (2)	B_{TBA}	7.0
(3)	$F_{ref,TBA}$	0.21
	E_{TBA}	18
	K_{H_2O}	1.5

[a] Ref. [10].
[b] Ref. [8].

3.2. Activity coefficient model

Honkela et al. [8,10] used Dortmund-modified UNIFAC [11] in calculating the liquid phase activity coefficients for their modelling work. Dortmund-modified UNIFAC is a predictive method that calculates the activity coefficients based on interactions of molecules and their subgroups. The same thermodynamic method is preferred in reactor simulations as is used in the kinetic modelling. Even though there are methods that are more suitable for hydrocarbon–alcohol systems, and that are based on experimental data, such as the Wilson method [12], preliminary simulations indicated that the results obtained by Dortmund-modified UNIFAC correspond better to the measurements than the ones made with other methods. Therefore, Dortmund-modified UNIFAC was used in the simulations.

3.3. Fluid properties

Parameters for liquid molar volume correlation by Lyckman et al. [13] were taken from the DIPPR database [14]. Enthalpies of formation and correlations for viscosities, conductivities and heat capacities were taken from Perry and Green [15].

4. Reactor model 2—hardware specific equations

4.1. Catalyst bed

According to the results of Honkela et al. [8,10], internal mass transfer is not a limiting factor concerning the reaction rates and therefore needs not to be included in the reactor model. External mass transfer was also found negligible in a CSTR, but this observation does not directly apply for a packed bed reactor. External mass transfer resistance in a packed bed is caused by a stagnant layer, which is formed outside a catalyst particle. However, as is discussed later in this chapter, this effect is negligible at these conditions and external mass transfer can be ruled out in the reactor model. Therefore, pseudohomogeneous approach is chosen for treating the catalyst bed. This simplifies the set of reactor equations and their mathematical treatment greatly.

Another important topic to address is whether radial and axial dispersion should be taken into account. In a strongly laminar flow region, as is the case here, backmixing (axial dispersion) is only caused by molecular diffusion, which in this case is very small compared to the fluid bulk flow rate. Therefore, axial dispersion was neglected.

Radial dispersion is mainly caused by turbulent effects. Here, the flow is strongly laminar ($5 < Re_p < 20$), so radial dispersion is partially neglected, and only diffusion and mixing due to the catalyst bed are included in the equations.

External heating/cooling induces radial temperature and concentration gradients in a tubular catalytic reactor. Therefore, it is necessary to include radial heat and mass transfer equations in a rigorous model. This leads to a system with partial differential equations (PDE's). Here, PDE's are converted into a system of ordinary differential equations (ODE's) by discretising the radial dimension of the catalyst bed.

The resulting set of ordinary differential equations for the system consists of enthalpy flow balances for each layer $i(1...n)$ (Eqs. (1)–(4)), material balances for each component j $(1...n_C)$ in each layer ((5)–(8)), and equations for heating fluid temperature ((15), (16), (18)) and wall temperatures ((17)).

The pressure drop in the reactor can be calculated by Ergun type correlation but the pressure drop in these studies is so small that it is approximated to zero, this assumption is based on low velocity of the fluid. The axial velocity profile varies only with the molar volume of the hydrocarbon mixture and as a function of the bed porosity ε.

The enthalpy flow $\dot{H}$ is the integrated variable instead of temperature T in the heat balances, and the heats of reaction are not included in the thermal balances as source terms. Since the enthalpy of the reaction mixture is calculated from enthalpies of formation and heat capacities at each integration point, the heats of reaction, often inaccurate and temperature-dependent, need not to be used, and the discrepancies in the heats of reaction for dimerisation reported in the literature [8,16] are eliminated. Heat is transferred to the catalyst bed only by conduction from adjacent layers of catalyst and by convection from inner and outer walls. The enthalpy balances for the layer next to the thermowell, here numbered as the first layer with subscript 1, have form of

$$\frac{\mathrm{d}\dot{H}_1}{\mathrm{d}z} = \pi\varepsilon\left(\alpha_w d_o(T_w - T_1) + \lambda_{er} d_2 (T_2 - T_1)\frac{n}{d_i - d_o}\right), \quad (1)$$

where α_w, λ_{er} and d_i and d_o are the wall heat transfer coefficient, the effective radial thermal conductivity and the inner and outer catalyst bed diameters, respectively. The enthalpy balance for the layer next to the tube outer wall is

$$\frac{\mathrm{d}\dot{H}_{n(\max)}}{\mathrm{d}z} = \pi\varepsilon\left(\alpha_w d_i(T_w - T_n) + \lambda_{er} d_2 (T_{n-1} - T_n)\frac{n}{d_i - d_o}\right), \quad (2)$$

and for intermediate layers

$$\frac{\mathrm{d}\dot{H}_i}{\mathrm{d}z} = \frac{\pi\varepsilon\lambda_{er} n}{d_i - d_o}(d_n(T_{i-1} - T_i) - d_{i+1}(T_{i+1} - T_i)). \quad (3)$$

The enthalpy balances have initial condition for layer i

$$(\dot{H}_i)_{z=0} = \dot{H}_{i,0} \quad (4)$$

In the material balances for each component j $(1...n_c)$ in each layer ((5)–(8)), the differential terms consist of mass transfer by diffusion between adjacent catalyst layers, and reaction term. The material balances for the layer next to the thermowell have form of

$$\frac{\mathrm{d}\dot{n}_{1,j}}{\mathrm{d}z} = \frac{D_{er}\varepsilon\pi d_2 n}{d_i - d_o}(C_2 - C_1) - r_j\rho_B\frac{\pi}{4}\varepsilon(d_2 - d_i)^2, \quad (5)$$

where $\dot{n}_{i,j}$, D_{er}, C_j, r_j and ρ_B are the molar flow of component j in layer i, the effective radial diffusivity, the concentration of component j, the reaction rate of component j and the bulk density of the fluid, respectively. The remaining material balances are

$$\frac{\mathrm{d}\dot{n}_{n,j}}{\mathrm{d}z} = \frac{D_{er}\varepsilon\pi d_i n}{d_i - d_o}(C_{n-1,j} - C_{n,j}) - r_j\rho_B\frac{\pi}{4}\varepsilon(d_o - d_{n-1})^2 \quad (6)$$

for the layer next to tube outer wall and

$$\frac{\mathrm{d}\dot{n}_{i,j}}{\mathrm{d}z} = \frac{D_{er}\varepsilon\pi n}{d_i - d_o}(d_i(C_{i-1} - C_i) + d_{i+1}(C_{i+1,j} - C_{i,j})) - r_j\rho_B\frac{\pi}{4}\varepsilon(d_i - d_{i-1})^2 \quad (7)$$

for the intermediate layers. The material balances have initial condition for layer i and component j

$$(C_{i,j})_{z=0} = C_{i,j,0} \quad (8)$$

Radial heat transfer is described by the effective radial heat conductivity, λ_{er}, and the wall heat transfer coefficient, α_w [17,18]. Radial mixing between the layers is caused by flow through the catalyst bed and diffusion of the components. In terms of mass transfer, radial mixing is modelled using the effective radial diffusivity D_{er}.

Several empirical correlations for λ_{er} for low Reynolds numbers and liquid phase reaction mixture were found from the literature [19–22]. None of these correlations was fitted for systems with a particle Reynolds numbers below 20, so a more fundamental approach for λ_{er} was used. λ_{er} consists of static part λ_{er}^0 and dynamic part λ_{er}^t.

$$\lambda_{er} = \lambda_{er}^0 + \lambda_{er}^t \quad (9)$$

Static contribution can be approximated as a volume average from fluid and catalyst conductivities

$$\frac{1}{\lambda_{er}^0} = \frac{1}{\lambda_g} + \frac{1}{\lambda_{cat}} \quad (10)$$

where λ_g and λ_{cat} are the fluid and catalyst thermal conductivities, respectively, and ε is the bed void fraction.

The dynamic part of the term is based on effective axial diffusion caused by turbulence and flow through catalyst bed

$$\frac{\lambda_{er}^t}{\lambda_g} = aPrRe = \frac{a\rho v D_P}{C_P} \quad (11)$$

Zehner and Schlünder [23] propose an expression for term a in (11) of form

$$a = \frac{0.14}{1 + 46\left(\frac{d_P}{d_o}\right)^2}, \quad (12)$$

but their experiments were made with gaseous fluid. With Eq. (12), value of a would be 0.12 for this system. Dekhtyar et al. [24] state that a value of 0.1 can be used for a in most conditions with an error margin of ±20%, and that value is used here.

λ_{er} was calculated individually for each layer, and average values were used for heat transfer between two layers.

Dekhtyar et al. studied the heat transfer in packed beds at low Reynolds number with liquid phase flow. For wall heat transfer coefficient, they state that at inertial flow mode ($Re_P < 80$), the

effect of the heat transfer resistance of the stagnant flow layer close to the walls becomes negligible. Analogously, external mass transfer resistance is caused by this stagnant layer around the catalyst particles, and the effect of it can, in the absence of the layer, be ruled out of the calculations. Film thickness calculations reveal that this in fact is the case, the film thickness at these conditions become so large that the entire fluid can be considered to be within the film.

The wall heat transfer coefficient α_w is generally used to describe this wall zone resistance, and in the absence of that resistance, a large value can be assigned for α_w and only λ_{er} is then used to describe the heat transfer inside the catalyst bed. The layers next to the wall are assumed to have the same temperature with the wall. This is important for the case in this study, since discretisation of the radial dimension conflicts with the use of α_w/λ_{er}-model, which also is not applicable with local bed porosities.

The dynamic part of the radial diffusivity of the bed, D_{er}, was calculated based on the analogy between heat and mass transfer, according to the following relation [25].

$$\lambda_{er}^{t} = \varepsilon \rho_g c_P D_{er} \tag{13}$$

where ρ_g is the fluid density and c_P the heat capacity of the fluid. Local averaged values were used for D_{er}. In the absence of turbulence, the effects of radial diffusion (of both heat and mass) are negligible. The static part of the effective radial diffusivity is molecular diffusion. At these conditions, diffusion coefficients are of magnitude 10^{-4} in comparison to the dynamic radial diffusivity. They can therefore be safely neglected and are not included in this model.

Daszkowski and Eigenberger [26] claim that, if radial variation in porosity is neglected, the calculated values for α_w and λ_{er} have 20–40% error in comparison to the real values. The bed porosity closer to the walls is significantly higher than in the middle of the catalyst section. The flow is thus higher in regions close to the walls. This phenomenon is called channelling and bypassing [27–30]. Here, the catalyst section is annular, and the flow will therefore be channelled to the vicinity of both inner and outer tube walls. The porosity profile after Winterberg and Tsotsas [31] for annular geometry is as follows:

$$\varepsilon = \varepsilon_{ave}(1 + 1.36\, e^{-5(R_o - R)/d_P}),\ R \geq \frac{R_o}{2}$$
$$\varepsilon = \varepsilon_{ave}(1 + 1.36\, e^{-5(R - R_o)/d_P}),\ R < \frac{R_o}{2} \tag{14}$$

where ε_{ave} is the average porosity of the bed and R_o is the radius of the reactor tube. R in Eq. (14) is taken to be in the middle of the discretised layer. Fig. 2 shows the porosity profile in the catalyst bed as a function of radius.

4.2. Heating coil

The temperature for the counter-currently flowing heating fluid (T_{heat}) is calculated from Eq. (15)

$$\frac{\partial T_{heat}}{\partial z} = -\frac{\alpha_{hw} \pi d_{ext}}{\dot{m}_{heat} c_{P,\,heat}} (T_{heat} - T_{wall}) \tag{15}$$

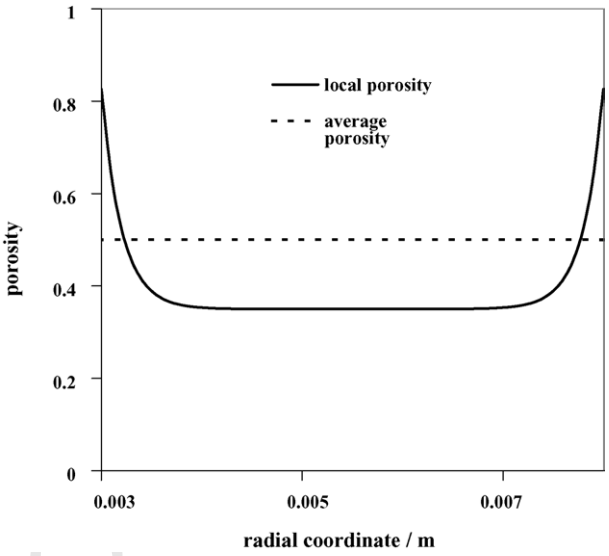

Fig. 2. Porosity of the bed as a function of reactor radius, d_P = 0.001 m, ε_{ave} = 0.5, R_i = 0.003 m, R_o = 0.008 m.

where α_{hw}, d_{ext}, $\dot{m}_{heat}$ and $c_{P,heat}$ are the heat transfer coefficient between the heating fluid and the reactor wall, the external diameter of the reactor tube, the heating fluid mass flow rate and the heating fluid heat capacity, respectively. The initial condition for Eq. (15) is

$$(T_{heat})_{z=0} = T_{heat,0} \tag{16}$$

4.3. Thermowell

The outer wall temperature T_{wall} follows the following second-order relation

$$\frac{d^2 T_{wall}}{dz^2} = 4\frac{\alpha_{hw}\pi d_{ext}(T_{heat} - T_{wall}) - \alpha_w \pi d_o (T_n - T_{wall})}{\lambda_{wall}\pi (d_{ext} - d_o)^2} \tag{17}$$

where λ_{wall} is the conductivity of the reactor wall.

Landon [32] studied the effects of a concentric axial thermowell in a tubular reactor. He made calculations in various conditions including sharp temperature gradients, and concluded that the temperature difference between the surrounding fluid and the thermowell did not exceed 0.8 K at any circumstances. Therefore, the thermowell temperature is assumed to be the same as that of the surrounding fluid in our calculations. However, in some experiments, at the beginning of the bed it can be seen that thermowell sheath conduction causes the fluid temperature to rise before the catalyst bed starts. The effect of the thermowell is also shown in the tunnelling of the fluid in the vicinity of the thermowell wall.

Now Eq. (15) has a form of

$$\frac{\partial T_{heat}}{\partial z} = -\frac{\alpha_{hw} \pi d_{ext}}{\dot{m}_{heat} c_{P,heat}} (T_{heat} - T_n) \tag{18}$$

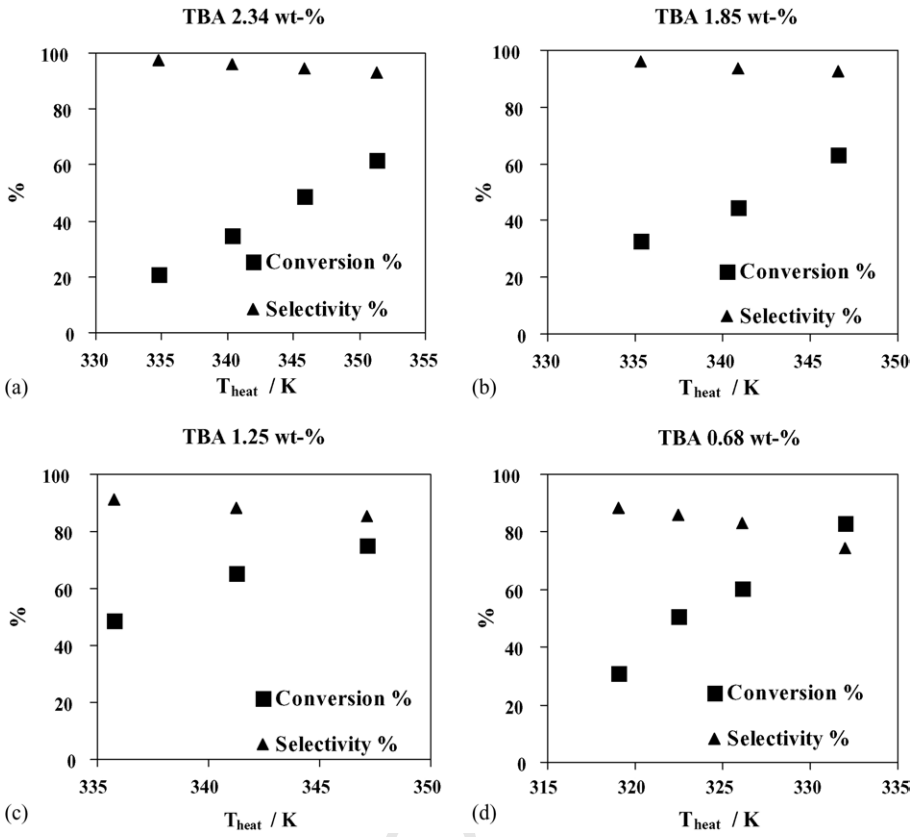

Fig. 3. (a–d) Test run results for one reactor; conversions and selectivities.

5. Results

5.1. Test run results

Table 2 lists the TBA concentrations in the feed and the heating coil temperatures for the test runs. Also measured isobutene conversions and selectivities into diisobutene are listed in Table 1 for each test run. Conversions and selectivities to diisobutene at various feed compositions as a function of the reactor feed temperature are plotted in Fig. 3a–d. As these figures suggest, the conversion increases and selectivity into diisobutene decreases when the reactor set temperature is increased. Also the concentration of TBA in the reactor feed plays an important role in isobutene oligomerisation. TBA decreases the reaction rate for all polymerisation reactions, and therefore the reaction system is more easily controlled and temperatures can be increased to gain higher conversions with better selectivity. Fig. 4a–d show selectivity and conversion of diisobutene as a function of the feed temperature at various TBA concentrations in the entrance of the first reactor. Here also the controllability of the reaction is a major contributor; if in the first reactor a good conversion is achieved, in the second reactor the set temperature can be raised and diisobutene yield maximised.

Temperature profiles inside the reactor thermowell were measured by moving four temperature probes gradually down the reactor axial length. Isobutene dimerisation ($\Delta H_r = -82.9$ kJ/mol [17] or $\Delta H_r = -107.2$ kJ/mol [9]) is a highly exothermic reaction as is the trimerisation reaction ($\Delta H_r = -157.4$ kJ/mol [9]), and the axial temperature rise may lead to reactor runaway in case of uncontrolled heat transfer. Both dimerisation and trimerisation reactions are rapid at the beginning of the reactor bed, and the coolant fluid is unable

Table 2
Feed concentrations and operating temperatures for test runs (two reactors in series)

Reactor	Feed IB (wt%)	Feed TBA (wt%)	Set temperature (K)	IB conversion (%)	DIB selectivity (%)
1	40.20	2.62	333.15	28.4	98.3
2	28.79	2.53	333.15	24.7	96.6
2	28.79	2.53	338.15	36.4	95.8
2	28.79	2.53	343.15	49.7	94.6
2	28.79	2.53	348.15	62.9	93.3
1	40.71	1.22	323.15	40.6	95.4
2	24.20	1.23	333.15	48.3	90.6
2	24.20	1.23	338.15	59.1	89.9
1	40.70	1.16	318.15	21.3	95.9
2	32.05	1.16	323.15	33.2	92.1
1	40.48	1.78	328.15	30.5	96.9
2	28.13	1.99	333.15	33.4	96.5
2	28.13	1.99	338.15	49.3	94.7
2	28.13	1.99	343.15	60.2	93.6
2	25.82	0.68	317.15	34.9	88.0
2	25.82	0.68	320.15	49.4	86.8
2	25.82	0.68	323.15	62.2	82.7

The catalyst bed length was 0.431 m for reactor 1 and 0.592 m for reactor 2. Average flow rate for all experiments was 280 g/h.

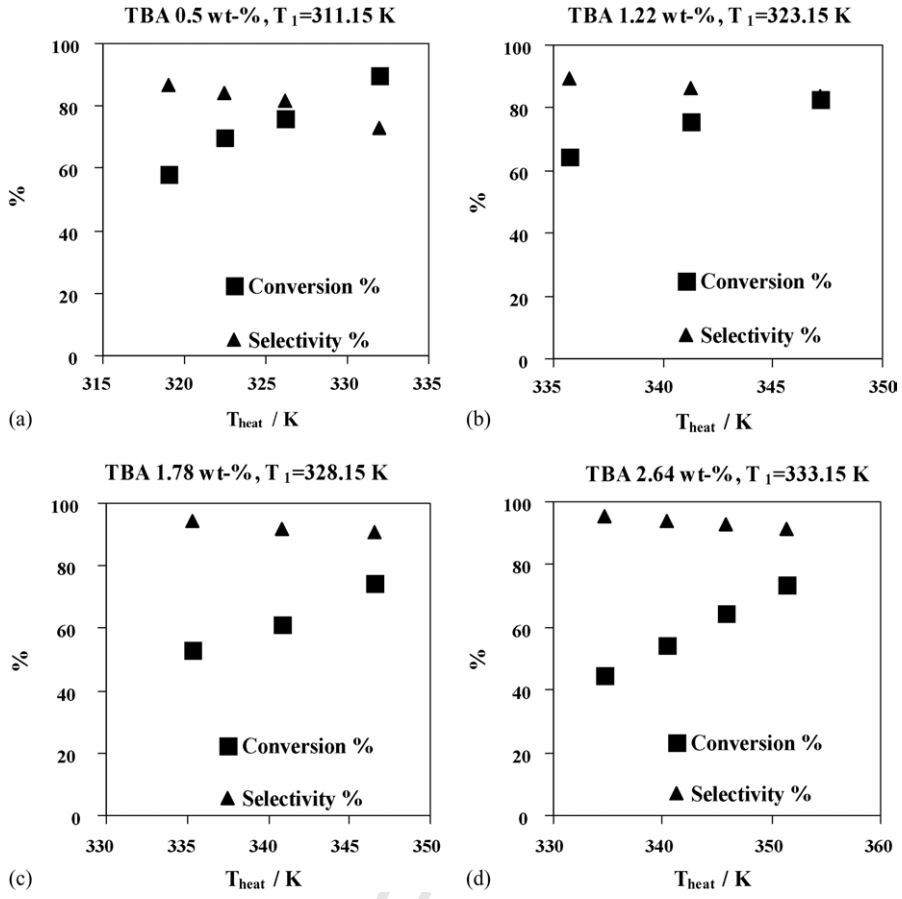

Fig. 4. (a–d) Test run results for two reactors in series; conversions and selectivities.

to keep the temperature profile flat. Over 25 K temperature rises were measured, yet in those experiments the reactor was operated very close to runaway conditions.

5.2. Simulated results

The level of radial discretisation is a trade-off between accuracy of the model and calculation time. One rule of thumb is that the thickness of a discretised layer should at least be equal to the diameter of the catalyst particle. Here, the average particle size was $d_{P,ave}$ = 0.8 mm, therefore the maximum amount of discretised layers is six, resulting from dividing the thickness of the bed in the annulus, 5 mm, by the average catalyst diameter.

Simulations with different discretisation levels support this rule of thumb; the quality of the model prediction is not markedly improved when the bed is divided into more than six radial layers.

Measured isobutene and TBA conversions together with selectivities into diisobutene and maximum thermowell temperatures are plotted against corresponding simulated values in Fig. 5a–d.

For both conversion and selectivities, the general trend of the simulated values seems to coincide well with the measured values. Predicted TBA conversions, however, seem to differ from measured values. Reasons for that, addressed in the next chapter, might include mass transfer resistance and absorption and desorption of both TBA and water as polar components into and from the ion exchange resin. The effect of TBA decomposition on the dimerisation reaction is reduced by the fact that also water operates as a selectivity-improving agent.

Most of the models for calculating the radial thermal conductivity presented in the literature, empirical or semi-empirical, are based on the experimental results in a system with turbulent fluid and often with a gaseous reaction mixture. At high Reynolds number and turbulent conditions the dynamic term of Eq. (9) becomes dominant. Turbulence also improves radial mixing inside the reactor, and therefore turbulent conditions are usually preferred when operating such reactors. Here, however, the particle Reynolds number does not exceed 10 (20 in the vicinity of the wall boundary) in any of the test runs, so the flow is laminar. In Eq. (9), this results in equally significant dynamic and static term.

Fig. 6a–c plot axial temperature profiles inside the thermowell, and in Fig. 6d–f, simulated radial temperature profiles are plotted at various points of the reactor axis. Both the maximum bed temperatures and axial locations of temperature maximums are accurately predicted. The average error in temperature maximums is 0.4 K.

Since heat is transferred by conductance, and no temperature jump occurs at the wall boundary layer, the radial temperature variations are as large as the axial ones. Therefore, it can be concluded that two-dimensional model is necessary for accurately

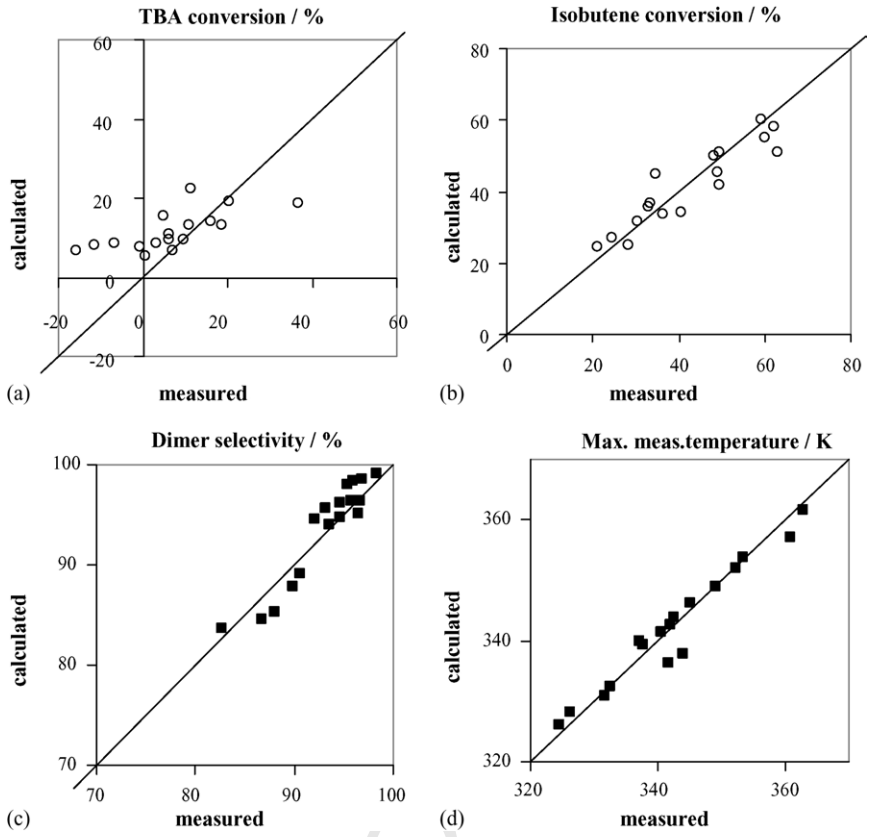

Fig. 5. Comparison between measured and calculated TBA conversions (a), isobutene conversions (b), diisobutene selectivities (c) and maximum bed temperatures (d).

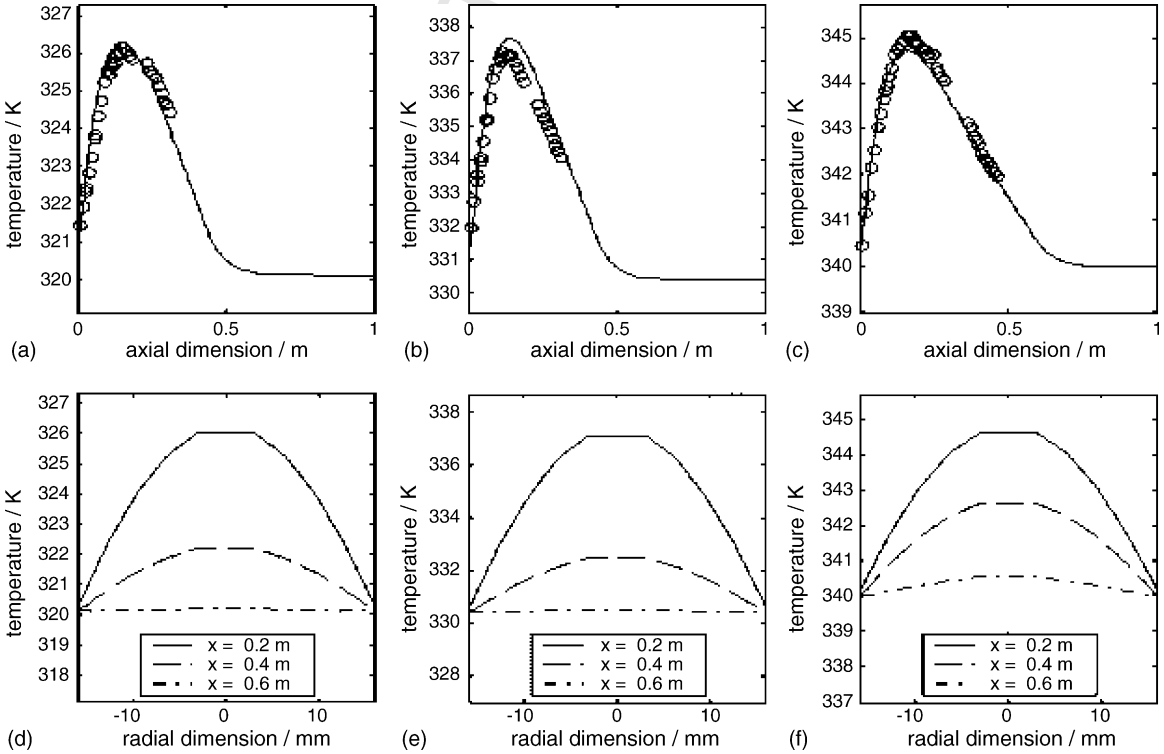

Fig. 6. (a–c) Axial temperature profile of the catalyst bed; measured (◯) and calculated (—) axial temperature; (d–f) radial temperature profiles at (—) $x = 0.1$ m, (– –) $x = 0.2$ m and (– · –) $x = 0.3$ m, x = position at the reactor axis measured from the beginning of the catalyst bed.

predicting the reactor performance. Furthermore, dimerising isobutene in laminar flow region in an externally cooled tubular reactor can not be seen as an industrially interesting option, since due to poor radial conductivity, increasing the radius of the reactor would increase the risk of reaction runaway at the centre-regions of the tube and catalyst bed. Multitubular reactors would solve the problem of large reactor radius, but they are expensive to build and the packing of the catalyst often complicated. The packing densities in each tube have to be equal in order to achieve equal flow rate in each tube.

6. Discussion

Possible causes for errors in the temperature profiles include thermal oil flow rate, heat losses to surrounding air from the heating coil, errors in the inlet temperature of the fluid, analytical errors in the feed compositions, etc. Taking these factors into account, the model performs the task of temperature profile prediction well.

Measured temperature rise in the entrance of the reactor is for some experiments sharper than the calculated one. Fluid maldistribution in the bed entrance may also be one reason for slower calculated initial reaction rates. The catalyst shrinks when water and TBA is desorbed from it, and thus leaves an empty section at the top of the reactor tube. The flow channels in the vicinity of the walls, and has higher superficial velocity and hence better mixing at the near-wall regions of the bed. Therefore, the heat is not transferred through the catalyst bed centre at the beginning of the bed. Here, the superficial velocities are between 1 and 2 mm/s, so flow channelling is unlikely to occur in significant amount.

In some test runs with no water in the feed mixture, negative TBA conversions were observed. Honkela et al. [8] made their kinetic experiments in a batch reactor, and chemical equilibrium should be well predicted by their kinetics, but at some TBA conversions the values predicted by our model were different than the measured ones. Thus, it is likely that the some steady states obtained were actually only “pseudo” steady states, with absorption and desorption of water and TBA between catalyst and reaction mixture taking place. Therefore, the steady-state model could not predict the TBA conversions accurately for all test runs.

The effect of dynamic sorption of polar components is small in terms of isobutene conversion, since the oligomerisation reactions have the highest sensitivity towards the initial concentration of TBA. Furthermore, it can be assumed that the beginning of the catalyst bed would be in equilibrium or at least close to it, and the highest rates of sorption would be found in the latter parts of the catalyst bed.

7. Conclusions

Isobutene dimerisation into diisobutene was studied in miniplant-scale reactors with a diameter of 0.016 m. TBA decomposition and further oligomerisation of diisobutene into triisobutene were additional side reactions considered. The reaction took place in liquid phase in the presence of solid cation exchange resin.

Once-through yields of up to 65% were measured for diisobutene. TBA was used as a selectivity-improving agent. Increasing the feed TBA content increases the selectivity but also decreases the conversion of isobutene.

The oligomerisation reactions of isobutene are highly exothermic, and sharp temperature gradients and axial temperature variations of over 25 K were observed in the reactors. External temperature control induced radial temperature and concentration gradients inside the catalyst bed. Knowing the temperatures inside the reactor is important not only to prevent potentially hazardous reaction runaways, but also in terms of catalyst stability, which in this case is compromised in high temperatures.

The experiments were modelled using a two-dimensional tubular reactor model including equations for thermowell and external heat transfer. Strong axial temperature variations were found inside the reactor with the two-dimensional model. No commercial software (to our best knowledge) has the option of two-dimensional treatment of the reactor, so a tailor-made model for the particular reactor used in the experiments was constructed.

At laminar flow regime, the thermal resistance of the wall layer becomes negligible, and hence only effective radial conductivity was used to describe the heat transfer in the catalyst bed. Temperature variations and peak locations inside bed were well described with this model.

The results in terms of conversion and selectivity of isobutene into diisobutene were rather accurate. Dynamic absorption of polar components in the catalyst resin was found to affect the measured TBA conversions to some extent, and the steady-state model could not predict the TBA conversions accurately for all test runs.

Acknowledgement

Funding from Fortum Oil and TEKES (The national technology agency of Finland) is gratefully acknowledged.

Appendix A. Nomenclature

a_i	activity of component i
c_P	heat capacity of the reactor fluid (J/mol K)
$c_{P,heat}$	heat capacity of the heat transfer fluid (J/kg K)
$C_{i,j}$	concentration of component j in layer i (mol/m^3)
D_{er}	effective radial diffusivity (m^2/s)
d_{ext}	external diameter of the reactor tube (m)
d_i	external diameter of the thermowell (m)
d_{int}	internal diameter of the thermowell (m)
d_j	outside diameter or layer j (m)
d_o	internal diameter of the reactor tube (m)
d_P	catalyst diameter (m)
d_R	reactor tube diameter (m)
$d_{P,ave}$	average catalyst diameter, average particle size (m)
$\dot{H}_i$	enthalpy flow in layer i (J/mol s)
ΔH_r	enthalpy of reaction (J/mol)
l_R	reactor length (m)

$\dot{m}_{heat}$ mass flow of the heat transfer fluid (kg/s)
$\dot{n}_{i,j}$ molar flow of component j in layer i (mol/s)
n number of discretised layers in radial dimension of the catalyst bed
n_C number of components
Pr Prandtl number, $Pr = \mu c_P/\lambda_g$
R radius (m)
Re Reynolds number, $Re = \rho_g v d_R/\mu$
Re_P Reynolds number, based on the surface velocity of the fluid, $Re_P = \rho_g v d_P/\mu$
R_o reactor tube inside radius (m)
r_j reaction rate of component j (mol/s $kg_{dry\ catalyst}$)
T temperature (K)
T_{heat} temperature of the heating fluid (K)
T_{wall} temperature of the reactor tube wall (K)
z axial dimension (m)

Greek letters

α_{hw} heat transfer coefficient between heating fluid and reactor wall (W/m^2 K)
α_w wall heat transfer coefficient (W/m^2 K)
ε porosity of the catalyst bed
ε_{ave} average porosity of the catalyst bed
ε_w local porosity of the catalyst bed at the vicinity of the wall, approximated as 1.0
λ_{er} effective radial thermal conductivity (W/m K)
λ_{cat} thermal conductivity of the catalyst (W/m K)
λ_g thermal conductivity of the reaction fluid (W/m K)
λ_{wall} wall heat conductivity (W/m K)
λ^0_{er} static contribution to the effective radial thermal conductivity (W/m K)
λ^t_{er} dynamic contribution to the effective radial thermal conductivity (W/m K)
μ viscosity of the fluid (kg/m s)
ρ_B bulk density of the catalyst in the reactor (kg/m^3)
ρ_g density of the reaction fluid (kg/m^3)

References

[1] Executive order D-5-99 by the Governor of the State of California, 25 March 1999.
[2] Executive order D-52-02 by the Governor of the State of California, 15 March 2002.
[3] G. Scharfe, Convert butenes to high octane oligomers, Hydrocarbon Process. 52 (1973) 171.
[4] M. Honkela, A.O.I. Krause, Influence of polar components in the dimerization of isobutene, Catal. Lett. 87 (2003) 113.
[5] P. Hunszinger, H. Järvelin, M. Nurminen, R. Birkhoff, Case history: converting an MTBE unit to isooctane operation, Hydrocarbon Process. 82 (2003) 57.
[6] W.O. Haag, Oligomerization of isobutene on cation exchange resins, Chem. Eng. Prog. Symp. Ser. 63 (1967) 140.
[7] P. Lievo, M. Almark, V.-M. Purola, A. Pyhalahti, J. Aittamaa, Miniplant, effective means to develop and design new processes, in: Annual Meeting Archive—American Institute of Chemical Engineers, Indianapolis, IN, United States, November 3–8, 2002, pp. 2010–2032.
[8] M. Honkela, T. Ouni, O. Krause, Thermodynamics and kinetics of the dehydration of *tert*-butyl alcohol, Ind. Eng. Chem. Res. 43 (2004) 4060.
[9] R. Alcantara, E. Alcantara, L. Canoira, M.-J. Franco, M. Herrera, A. Navarro, Trimerization of isobutene over Amberlyst-15 catalyst, React. Funct. Polym. 45 (2000) 19.
[10] M.L. Honkela, A.O.I. Krause, Kinetic modeling of the dimerization of isobutene, Ind. Eng. Chem. Res. 43 (2004) 3251.
[11] U. Weidlich, J. Gmehling, A modified UNIFAC model. 1. Prediction of VLE, HE, and g^E, Ind. Eng. Chem. Res. 26 (1987) 1372.
[12] G.M. Wilson, Vapor–liquid equilibrium. XI. A new expression for the excess free energy of mixing, J. Am. Chem. Soc. 86 (1964) 127.
[13] E.W. Lyckman, C.A. Eckert, J.M. Prausnitz, Generalized liquid volumes and solubility parameters for regular solution application, Chem. Eng. Sci. 20 (1965) 703.
[14] R.L. Rowley, W.V. Wilding, J.L. Oscarson, N.A. Zundel, T.L. Marshall, T.E. Daubert, R.P. Danner, DIPPR® Data Compilation of Pure Compound Properties Design Institute for Physical Properties, AIChE, New York, 2002.
[15] R.H. Perry, D.W. Green, Perry's Chemical Engineers' Handbook, seventh ed., McGraw-Hill, New York, 1997.
[16] M. Marchionna, M. Di Girolamo, R. Patrini, Light olefins dimerization to high quality gasoline components, Catal. Today 65 (2001) 397.
[17] E.-U. Schlünder, E. Tsotsas, Wärmeübertragung in Festbetten, durchmischten Schüttgütern und Wirbelschichten, Georg Thieme, Stuttgart, Germany, 1988.
[18] F. Froment, K.B. Bischoff, Chemical Reactor Analysis and Design, second ed., Wiley, New York, 1990.
[19] A.G. Dixon, D.L. Cresswell, Theoretical prediction of effective heat transfer parameters in packed beds, AIChE J. 25 (1979) 663.
[20] J.B. Agnew, O.E. Potter, Heat transfer properties of packed tubes of small diameter, Trans. Inst. Chem. Eng. 48 (1970) T15.
[21] R. Bauer, Effective radial thermal conductivity of gas-permeated packed beds containing particles of different shape and size distribution, VDI-Forschungsheft 582 (1977) 39.
[22] A. Stankiewicz, Advances in modeling and design of multitubular fixed-bed reactors, Chem. Eng. Technol. 12 (1989) 113.
[23] P. Zehner, E. Schluender, Thermal conductivity of packings at moderate temperatures, Chem. Eng. Technol. 42 (1970) 933.
[24] R.A. Dekhtyar, D.P. Sikovsky, A.V. Gorine, V.A. Mukhin, Heat transfer in a packed bed at moderate values of the Reynolds number, High Temp. 40 (2002) 693.
[25] A.G. Dixon, L.A. Labua, Wall-to-fluid coefficients for fixed bed heat and mass transfer, Int. J. Heat Mass Transfer. 28 (1985) 879.
[26] T. Daszkowski, G. Eigenberger, A revaluation of fluid flow, heat transfer and chemical reaction in catalyst filled tubes, Chem. Eng. Sci. 47 (1992) 2245.
[27] C.E. Schwartz, J.M. Smith, Flow distributions in packed beds, Ind. Eng. Chem. 45 (1953) 1209.
[28] P.H. Calderbank, L.A. Pogorski, Heat transfer in packed beds, Trans. Inst. Chem. Eng. 35 (1957) 195.
[29] E.U. Schlünder, On the mechanism of mass transfer in heterogeneous systems—in particular in fixed beds, fluidized beds and on bubble trays, Chem. Eng. Sci. 32 (1977) 845.
[30] H. Martin, Low Peclet number particle-to-fluid heat and mass transfer in packed beds, Chem. Eng. Sci. 33 (1978) 913.
[31] M. Winterberg, E. Tsotsas, Modelling of heat transport in beds packed with spherical particles for various bed geometries and/or thermal boundary conditions, Int. J. Therm. Sci. 39 (2000) 556.
[32] V.G. Landon, Temperature correction for packed bed multitubular reactors with concentric axial thermowells, Comput. Chem. Eng. 20 (1996) 475.